Published in final edited form as:

Circulation. 2019 November 19; 140(21): 1720–1733. doi:10.1161/CIRCULATIONAHA.118.037968.

MCUB regulates the molecular composition of the mitochondrial calcium uniporter channel to limit mitochondrial calcium overload during stress

Jonathan P. Lambert, PhD[1], **Timothy S. Luongo, PhD**[1], **Dhanendra Tomar, PhD**[1], **Pooja Jadiya, PhD**[1], **Erhe Gao, MD, PhD**[1], **Xueqian Zhang, PhD**[1], **Anna Maria Lucchese, MS**[1], **Devin W. Kolmetzky, BS**[1], **Neil S. Shah, BS**[1], **John W. Elrod, PhD**[1]

[1]Center for Translational Medicine, Lewis Katz School of Medicine at Temple University, Philadelphia, PA, 19140

Abstract

Background: The mitochondrial calcium uniporter (mtCU) is a ~700 kD multi-subunit channel residing in the inner mitochondrial membrane (IMM) required for mitochondrial Ca^{2+} ($_{m}Ca^{2+}$) uptake. Here we detail the contribution of MCUB, a paralog of the pore-forming subunit - MCU, in mtCU regulation and function and for the first time investigate MCUB's relevance to cardiac physiology.

Methods: We created a stable *MCUB* knockout cell line (*MCUB*$^{-/-}$) utilizing CRISPR-Cas9n technology and generated a cardiac-specific, tamoxifen-inducible MCUB mutant mouse (CAG-CAT-MCUB x MCM; MCUB-Tg) for in vivo assessment of cardiac physiology and response to ischemia-reperfusion (IR) injury. Live cell imaging and high-resolution spectrofluorometery were employed to determine intracellular Ca^{2+} exchange and size-exclusion chromatography, blue native page and immunoprecipitation studies were utilized to determine the molecular function and impact of MCUB on the high-molecular weight mtCU complex.

Results: Using genetic gain- and loss-of-function approaches we show that MCUB expression displaces MCU from the functional mtCU complex and thereby decreases the association of MICU1 and MICU2 to alter channel gating. These molecular changes decrease MICU1/2-dependent cooperative activation of the mtCU thereby decreasing $_{m}Ca^{2+}$ uptake. Further, we show that MCUB incorporation into the mtCU is a stress-responsive mechanism to limit $_{m}Ca^{2+}$ overload during cardiac injury. Indeed, overexpression of MCUB is sufficient to decrease infarct size following IR injury. However, MCUB incorporation into the mtCU does come at a cost, as acute decreases in $_{m}Ca^{2+}$ uptake impairs mitochondrial energetics and contractile function.

Conclusions: In summary, we detail a new regulatory mechanism to modulate mtCU function and $_{m}Ca^{2+}$ uptake. Our results suggest that MCUB-dependent changes in mtCU stoichiometry is a prominent regulatory mechanism to modulate $_{m}Ca^{2+}$ uptake and cellular physiology.

Correspondence: John W. Elrod, PhD, Center for Translational Medicine, 3500 N Broad St, MERB 949, Philadelphia, PA 19140, Office: (215) 707-5480, Lab: (215) 707-9144, Fax: (215) 707-9890, elrodlab.org.

Disclosures: The authors have no conflicts of interest, financial or otherwise, to report.

Keywords

mitochondria; calcium regulation; calcium signaling; calcium channel; oxidative phosphorylation; mitochondrial calcium uniporter channel; MCU; MCUB; MICU1; mitochondrial biology; ischemia reperfusion injury; cardiac function

Introduction

The mitochondrial calcium uniporter (mtCU) is an inward-rectifying, high-molecular weight (MW) channel that resides in the inner mitochondrial membrane and is necessary to facilitate calcium (Ca^{2+}) uptake into the mitochondrial matrix[1–3]. Ca^{2+} flux through the mtCU is driven by the large electrochemical gradient (−180 mV) across the inner mitochondrial membrane that is generated by the electron transport chain (ETC)[2]. Physiologically, the mtCU is required for the activation of calcium-dependent dehydrogenases involved in oxidative phosphorylation. In addition, during stress the mtCU mediates $_{m}Ca^{2+}$ overload, which is a prominent activator and sensitizer of the mitochondrial permeability transition pore (MPTP) resulting in cell death[4]. Our lab and others, have previously shown that genetic modulation of either $_{m}Ca^{2+}$ uptake[5, 6] or efflux[7] is a powerful way to limit cardiomyocyte death in the context of ischemia-reperfusion (IR) injury and heart failure and therefore understanding the molecular regulation of these pathways holds therapeutic promise.

The mtCU consists of multiple components each with a unique role in channel regulation and function. *MCU* encodes the pore-forming subunit of the channel and is also the target of the MCU-inhibitor, ruthenium red – Ru360, a pharmacological inhibitor long known to inhibit mitochondrial Ca^{2+} uptake ($_{m}Ca^{2+}$)[1, 3, 8]. Loss of MCU completely ablates all channel function resulting in no acute $_{m}Ca^{2+}$ uptake[5, 6, 9]. MCU is thought to form homooligomers with a highly-conserved ‘DIME’ sequence motif serving as the ion selectivity filter and the second transmembrane domain contributing to the formation of a hydrophilic pore spanning the IMM[10]. *Mitochondrial Calcium Uptake 1* (*MICU1*) was the first component of the complex identified through comparative physiology and evolutionary genomic approaches[11]. *MICU1* contains two Ca^{2+}-binding EF-hands and is reported to be a channel gatekeeper by maintaining closure of the mtCU at low cytosolic Ca^{2+} ($_{c}Ca^{2+}$) levels[12–14]. *MICU1* also contributes to the cooperative activation of the channel by increasing uptake rates at high $_{c}Ca^{2+}$ levels[13, 15]. *MICU2* is a gene paralog of *MICU1* and is reported to calibrate MICU1-mediated regulation of the uniporter complex[16, 17]. *SMTD1* encodes for Essential MCU Regulator (EMRE), which also appears to be required for mtCU function, suggesting that the minimal functional channel may consist of MCU and EMRE[18]. EMRE is reported to be necessary for MICU1/MICU2 interactions with MCU and therefore may also indirectly contribute to channel gating[18,19]. *MCUR1* (Mitochondrial Calcium Uniporter Regulator 1) has been identified as another component that modulates mtCU function, possibly serving as a scaffold for channel formation[20]. *MCUB* was recently put forth as a possible mtCU constituent because of its close sequence similarity to *MCU*, encoding for a protein that shares ~50% aa homology and contains two similar transmembrane domains linked by an identical DIME motif[21]. MCUB was found to form

hetero-oligomers with MCU and expression of MCUB alone in a lipid-bilayer resulted in little to no Ca^{2+} exchange across an artificial membrane[21]. This earlier study strongly suggests MCUB is a bona fide mtCU constituent that exerts a negative effect on Ca^{2+} uptake, but it remains unclear whether MCUB directly influences Ca^{2+} permeation of the pore or regulates the mtCU through some other mechanism. Also, MCUB's physiological relevance remains unresolved. Here using genetic loss- and gain-of-function approaches we report that MCUB modulates the stoichiometry of mtCU subunits to fine-tune $_{m}Ca^{2+}$ uptake. Further, while MCUB is absent from the mtCU in homeostatic hearts, it is a prominent regulator of cardiac function during stress by integrating into the uniporter complex; significantly impacting mitochondrial energetics and reducing $_{m}Ca^{2+}$ overload during injury.

Main Methods

For detailed materials and methods please refer to the online-only Data Supplement. All data presented here are freely available upon any reasonable request.

Animal Studies:

All animal experiments were formally approved and in accordance with institutional guidelines established by the Temple University Institutional Animal Care and Use Committee, which follows the Association for Assessment and Accreditation of Laboratory Animal Care International guidelines. All mice were on the C57/BL6N background strain. Female and male mice were used for all studies unless otherwise noted in a specific experimental assay. For this study, approximately 20 C57BL6N wild-type, 150 αMHC-MCM and 150 MCUB-Tg x αMHC-MCM mice were utilized. Whenever possible experiments were performed in a blinded fashion with randomization. For example, a lab technician ear-tagged and coded mice to mask the genotype from the experimenter. Surgical procedures and anesthetic agents utilized for each procedure are detailed in the description of each experimental procedure.

Generation of a stable *MCUB*$^{-/-}$ HeLa cell line

We generated a stable *MCUB* knockout HeLa cell line using CRISPR/Cas9n technology to target exon 1 of *MCUB* for genomic deletion following the protocol developed by the Zhang lab[22]. Detailed methods along with plasmids, guide RNAs, and qPCR primers/antibodies utilized to confirm gene deletion and loss of protein are listed in the online-only Data Supplement.

Generation of a cardiac-specific MCUB gain-of-function transgenic model

MCUB transgenic (MCUB-Tg) mutant mice were generated using a flox-stop strategy where mouse *Mcub* cDNA (CCDS 17839.1) was cloned into a custom CAG-loxP-CAT-loxP plasmid. Detailed methods about molecular cloning, selection of a transgenic lines and the tamoxifen protocol for Cre-dependent expression can be found in the Data Supplement. MCUB-Tg mice were crossed to cardiomyocyte-restricted Cre expressing mouse models (αMHC-Cre or αMHC-MerCreMer) for all experiments.

Size exclusion chromatographic analysis of the high molecular weight mtCU complex

2,500 μgrams of whole cell protein lysates or pure cardiac mitochondrial protein lysates prepared in RIPA lysis buffer were fractionated by gel filtration using fast protein liquid chromatography. All procedures were carried out as previously reported[20] and detailed methods can be found in the Data Supplement.

Blue Native Page Gel Electrophoresis

Purified cardiac mitochondria were incubated on ice for 20 minutes with Invitrogen 4x NativePAGE sample buffer with digitonin at a final concentration of 2%. Samples were then centrifuged at 18,000 x g for 30 minutes at 4 degrees Celsius. The supernatant was supplemented with G-250 sample additive at a final concentration of 0.25% and samples were then loaded for gel electrophoresis runs on an Invitrogen NativePAGE Novex Bis-Tris gel system. Gels were transferred for 18 hours at 4 degrees Celsius at 20 volts. Then immunoblotted with specified antibody.

Echocardiography

Transthoracic echocardiography of the left ventricle was performed and analyzed on a Vevo 2100 imaging system (VisualSonics) as previously reported[7] and detailed methodology can be found in the online-only Data Supplement.

Isolation of ACMs

ACMs were isolated from ventricular tissue as described previously[23]. All cells were used within 4 h of isolation.

Evaluation of $_{m}Ca^{2+}$ Uptake, Content, and $_{m}Ca^{2+}$ retention capacity experiments

All procedures were carried out as previously reported[7]. For detailed methods please refer to the online-only Data Supplement.

Mitochondria Isolation and Swelling Assay

Hearts were excised from mice and mitochondria were isolated as reported[24]. For the swelling assay, mitochondria were diluted in assay buffer, and absorbance (abs) was recorded at 540 nm every 5 s. 500 μM $CaCl_2$ was injected to induce swelling[25].

Adult mouse cardiomyocyte $_{i}Ca^{2+}$ and $_{m}Ca^{2+}$ transient recordings

Intracellular calcium dynamics in isolated ACMs were examined as previously described[7] and detailed methodology can be found in the online-only Data Supplement.

Mitoplast Patch-Clamp Analysis of MCU Current

Following mitochondrial isolation, mitoplasts were prepared for patch-clamp studies. I_{MCU} was recorded as previously described in detail[26].

Oxygen Consumption Assays

Detailed methodology has been previously reported[7] and can be found in the online-only Data Supplement.

Invasive hemodynamic measurements

All details are previously described[5] and detailed methodology can be found in the online-only Data Supplement.

Permanent ligation of the LCA and ischemia-reperfusion injury

LCA ligation and reperfusion was performed as previously described in detail[27]. Detailed methodology can be found in the online-only Data Supplement.

$_{c}Ca^{2+}$ and $_{m}Ca^{2+}$ flux in HeLa cells

Cells were transduced with AAV6-mito-R-GECO1 for 72 hours and live-cell imaging with a Zeiss microscope was performed to measure $_{m}Ca^{2+}$ exchange following histamine stimulation (100 μM). Cells were also loaded with the $_{i}Ca^{2+}$ indicator, Fluo4-AM, and imaged to monitor $_{c}Ca^{2}$ flux following histamine stimulation. Data were collected every 0.5 s and analyzed using Zen software.

Co-Immunoprecipitations

Plasmids encoding MCU, MCUB, MICU1, and MICU2 tagged with HA or FLAG were generated and transfected into COS7 cells for co-immunoprecipitations. Detailed methodology can be found in the online-only Data Supplement where methods about endogenous immunoprecipitations can also be found.

Statistical Analysis

All results are presented as mean ± SEM. Statistical analysis was performed using Prism 6.0 software (GraphPad). For comparisons between two groups, an unpaired, two-tailed t test was used. For groups of three or more a one-way ANOVA with Bonferroni correction was used. For grouped analyses, either multiple unpaired t-tests with correction for multiple comparisons using the Holm-Sidak method or two-way ANOVA with Tukey post-hoc analysis were performed. For all echocardiographic analysis two-way repeated-measures ANOVA was used with Sidak's post hoc analysis. Log-rank test was used for comparison of Kaplan-Meier survival curves.

Results

MCUB deletion alters mtCU formation, stoichiometry, and $_{m}Ca^{2+}$ uptake

To evaluate how MCUB contributes to mtCU function we generated a stable *MCUB* knockout HeLa cell line (*MCUB*$^{-/-}$) using CRISPR/Cas9n. We targeted exon 1 by employing a double nickase strategy[22] to avoid off-target genomic editing (Fig 1A). Following puromycin selection, clonal *MCUB*$^{-/-}$ cell lines were examined for loss of mRNA by qPCR and protein by Western blot analysis. Two clonal lines were found to be void of MCUB mRNA and protein; *line 2* was used in all subsequent experiments (Supp. Fig 1A). mRNA expression of mtCU subunits indicated that the ratio of MCU:MCUB in WT HeLa cells is ~3:1 (Supp. Fig 1B). Deletion of *MCUB* resulted in an increase in the expression of core mtCU subunits. Western blot analysis revealed that MCU expression increased ~2.7-fold and EMRE expression increased ~4.5-fold, as compared to wild-type

(WT) controls (Fig 1B). Complex V (CV-Sα) of the ETC served as a mitochondrial protein loading control. We next investigated if loss of MCUB altered the composition of the mtCU complex. WT and *MCUB*$^{-/-}$ cell lysates were fractionated in non-reducing conditions by size-exclusion, Fast Protein Liquid Chromatography (FPLC; Fig 1C–E). FPLC fractions were calibrated to known MW standards (Supp. Fig 1D–1E) and fractions 4–12 (corresponding to ~200–900 kD MW fractions) were collected, concentrated, and examined by Western blot under reducing conditions. MCUB was detected in high-MW fractions of WT HeLa cells, but undetected in *MCUB*$^{-/-}$ cells (Supp. Fig 1F). *MCUB* deletion increased the presence of MCU in the mtCU by ~2.5-fold with a significant increase in expression in high-MW fractions (~450–800 kD; Fig 1C). In addition, the channel regulators MICU1 and MICU2 displayed increased expression in the high-MW complex in *MCUB*$^{-/-}$ cells (Fig 1D, 1E). These results suggest that MCUB expression regulates overall mtCU formation and stoichiometry.

Given the dynamic changes in mtCU formation, we next investigated how MCUB expression impacts uniporter function. We evaluated $_{m}Ca^{2+}$ dynamics by transducing wild-type (WT) and *MCUB*$^{-/-}$ cells with adeno-associated virus (AAV) encoding mito-R-GECO1[28], a genetic calcium reporter targeted to the mitochondrial matrix, and monitored changes in fluorescence by live-cell imaging during histamine simulation, which mediates an Inositol trisphosphate receptor (IP3R) mediated increase in $_{c}Ca^{2+}$ (Fig 1F). Loss of MCUB increased the $_{m}Ca^{2+}$ amplitude by ~80%, suggesting *MCUB*$^{-/-}$ cells display increased $_{m}Ca^{2+}$ uptake (Fig 1G). To examine if alterations in $_{m}Ca^{2+}$ uptake impacted $_{c}Ca^{2+}$ signaling, cells were loaded with the reporter, Fluo4-AM, and live-cell imaging was performed during histamine treatment (Fig 1H). *MCUB* deletion decreased the $_{c}Ca^{2+}$ transient amplitude by ~35%, suggestive of enhanced mitochondrial buffering (Fig 1I).

We next evaluated if MCUB altered gating of the mtCU. WT and *MCUB*$^{-/-}$ cells were permeabilized; endoplasmic reticulum (ER) Ca^{2+} uptake inhibited with thapsigargin, and loaded with the ratiometric reporters Fura-FF and JC-1 to simultaneously record changes in Ca^{2+} flux and mitochondrial membrane potential ($\Delta\psi$). $_{m}Ca^{2+}$ uptake was monitored during incremental changes in bath Ca^{2+} [0.5 – 10 μM] (Supp. Fig 1G). The $_{m}Ca^{2+}$ uptake rate was quantified for 200s following each bolus of bath Ca^{2+} and exponentially fit to the Hill equation (Fig 1J). *MCUB*$^{-/-}$ cells exhibited increased $_{m}Ca^{2+}$ uptake rates across a wide range of Ca^{2+} concentration, with significant differences beginning at [Ca^{2+} > 3 μM]. Next, to examine if MCUB altered overall channel capacitance we patch-clamped whole mitoplasts and monitored current during a voltage ramping protocol (−160 mV to 80 mV) in the presence of Ca^{2+} (5 mM) (Fig 1K). Loss of MCUB significantly increased the current density (Fig 1L) suggesting an increase in overall functional mtCU. To see if the increase in current density and uptake-rate at high-Ca^{2+} impacted overall matrix content of free-Ca^{2+} we evaluated the release of $_{m}Ca^{2+}$ induced by FCCP (Fig 1M). Loss of MCUB trended to increased basal matrix Ca^{2+} content, but this did not reach statistical significance (Supp. Fig 1C and Fig 1N). Next, we performed $_{m}Ca^{2+}$ retention capacity (mCRC) experiments in our permeabilized cell system during repetitive boluses of 10 μM Ca^{2+} until loss of membrane potential (Fig 1O–P). *MCUB*$^{-/-}$ cells were able to withstand ~30% less bath Ca^{2+} load before collapse of $\Delta\psi$ indicating a decrease in mCRC and increase in susceptibility to permeability transition (Fig 1Q). These data suggest that *MCUB* deletion enhances overall

mtCU formation and/or increases cooperative activation and uptake-rate in high-Ca^{2+} conditions, both of which may predispose cells to $_{m}Ca^{2+}$ overload.

MCUB incorporates into the mtCU complex after injury

Aberrant $_{i}Ca^{2+}$ cycling is a key feature and contributor to the development and progression of cardiac injury[29]. We have previously shown that $_{m}Ca^{2+}$ overload contributes to IR-injury and heart failure progression[5, 7]. To discern changes in mtCU component expression we evaluated left ventricle mRNA expression 2d and 14d after permanent ligation of the left coronary artery (LCA) which induces a large myocardial infarction (MI). We found that *MCUB* expression was significantly increased 48h following MI, resulting in ~3-fold increase in MCUB/MCU expression. (Fig 2A). Next, we evaluated the high-MW mtCU for changes in MCUB expression following IR-injury. After IR-injury, mitochondria were isolated from ventricular tissue and fractionated by size-exclusion FPLC. Fractions ranging from ~200–900 kD were run under reducing conditions and immunoblotted for MCUB expression. Interestingly, MCUB was completely absent from the high-MW fractions of sham-operated hearts nor was MCUB detected in high-MW fractions of hearts subjected to 40 minutes of ischemia and 12 hours of reperfusion. However, 24 hours after reperfusion MCUB clearly detected in the ~600–800 kD fractions (Fig 2B).

Generation of a cardiac-restricted MCUB transgenic mouse model

To examine the physiological relevance of MCUB expression and incorporation into the mtCU in cardiac physiology and disease we generated a gain-of-function mouse model employing a flox-stop strategy where MCUB cDNA was cloned into a construct containing a CAG promoter followed by a floxed chloramphenicol acetyltransferase (CAT) to allow for Cre-driven deletion of CAT and expression of MCUB (Fig 2C). We characterized 10 founder lines for both leakiness (basal expression void of Cre) and level of expression following Cre-mediated activation by crossing founder lines to the cardiomyocyte-specific αMHC-Cre model (Supp. Fig 2A). After selection of a founder with tightly regulated expression we crossbred our MCUB transgenic mouse to the αMHC Mer-Cre-Mer (MCM) driver line[30] to enable conditional expression of MCUB in the adult heart (Fig 2C). Tamoxifen (tamox) was administered i.p. (25 mg/kg/d for 4d) to induce MCUB expression. One day following tamox treatment cardiac protein lysate was obtained to evaluate MCUB protein expression by Western blot analysis. We confirmed a significant increase in MCUB overexpression, which resulted in a ~15-fold increase in the MCUB:MCU ratio with no baseline change in the expression of other mtCU subunits (Fig 2D–F). Next, adult cardiomyocytes (ACMs) were isolated from MCUB-Tg x MCM and controls and $_{m}Ca^{2+}$ uptake was examined independently of intracellular calcium handling with simultaneous monitoring of mitochondrial membrane potential (Fig 2G). Overexpression of MCUB reduced the rate of $_{m}Ca^{2+}$ uptake by ~70% and similarly decreased the amount of Ca^{2+} taken up following a 5 μM bath-Ca^{2+} bolus (Fig 2H, 2I). To examine Ca^{2+} flux in intact cardiomyocytes we injected mice with AAV encoding the mitochondrial-targeted reporter, mitycam. ACMs were isolated and live-cell imaging was performed during pacing at 0.1 Hz to resolve individual $_{m}Ca^{2+}$ transients (Fig 2J). MCUB-Tg x MCM cardiomyocytes displayed a ~28% reduction in the peak amplitude of $_{m}Ca^{2+}$ transients during pacing (Fig 2K). The rate-of-decay, (Supp. Fig 2B) was not statistically different. To assess $_{C}Ca^{2+}$ transients, ACMs were isolated and

loaded with the Ca^{2+} reporter, Fluo-4, and paced at 1 Hz (Fig 2L–2M) (+/−) 100 nM isoproterenol. At baseline there was no significant difference in the peak-amplitude of $_{C}Ca^{2+}$ transients between groups, but we did note a slight ~20% increase in the $_{c}Ca^{2+}$ transient amplitude of isoproterenol-treated MCUB-Tg x MCM cardiomyocytes (Fig 2N). The rate-of-decay, (Supp. Fig 2C) was not statistically different.

Overexpression of MCUB reduces $_{m}Ca^{2+}$-overload and cardiac IR-injury

To examine how a MCUB-dependent decrease in $_{m}Ca^{2+}$ uptake impacted physiology, we evaluated cardiac function by echocardiography 1wk and 1m after transgene induction (post-tamox treatment). One week after MCUB expression fractional shortening was reduced by ~40% (Fig 3A) and LV end-diastolic and LV end-systolic diameters (LVEDD, LVESD) were significantly increased (Supp. Fig 3B, 3C). One month post-tamox treatment all echocardiographic parameters of MCUB-Tg x MCM mice returned to MCM control levels indicating the transient decrease in cardiac function elicited by MCUB expression was compensated for (Fig 3A, Supp. Fig 3B, 3C). Acute MCUB expression (1wk) elicited a slight increase in LV mass indicative of cardiac remodeling that was resolved at the 1m-time point (Supp. Fig 3H–I). At baseline, 1w, and 1m post-tamox treatment the heart rate was not different between groups (Supp. Fig 3A). IR results in pathogenic increases in $_{i}Ca^{2+}$ levels[31] and we have previously reported that MCU-mediated $_{m}Ca^{2+}$ overload is a significant contributor to cardiac injury via the induction of the mitochondrial permeability transition pore[5]. Given the transient cardiac dysfunction noted with MCUB overexpression we employed two protocols to examine how MCUB modulation of the mtCU impacted cardiac injury. LCA ligation (40m ischemia and 24h reperfusion) was performed 1wk (Protocol 1) and 1m (Protocol 2) after tamox treatment (Fig 3B). Surprisingly, in contrast to studies performed in the MCU cKO mouse model[5, 6], myocardial IR performed 1wk post-tamox resulted in substantial mortality of MCUB-Tg x MCM mice. 12/13 mice expressing MCUB died within a few minutes of ischemia (Fig 3C). In stark contrast, IR induced 1m after tamox treatment resulted in no difference in survival between MCM and MCUB-Tg x MCM mice (Supp. Fig 3J). In fact, MCUB expression significantly reduced infarct size per area-at-risk (AAR) by ~50%, as compared to MCM controls (Fig 3D, Supp. Fig 3K). No statistical difference in AAR/LV was observed confirming a similar ligation and ischemic zone in all hearts. We have previously reported that inhibition of mtCU-uptake is protective against IR-injury by lessening activation of the mPTP[5]. Therefore, we examined swelling (an indicator of mPTP activity) in ventricular mitochondria isolated from MCUB-Tg x MCM and control mice. Absorbance was monitored during the delivery of a 500 μM Ca^{2+} bolus (Fig 3E). Increased expression of MCUB reduced both the rate and extent of mitochondrial swelling induced by Ca^{2+} overload (Fig 3F,G).

MCUB expression impairs mitochondrial energetics and contractility during stress

Since acute MCUB expression resulted in a transient decrease in cardiac function 1w post-tamox we employed invasive hemodynamics to monitor LV function during isoproterenol (iso) infusion 1d after tamox administration (Fig 4A). Acute MCUB expression slightly depressed heart rate at a single dose of iso (Fig 4B). Overexpression of MCUB completely ablated iso-induced elevations in contractility (dP/dt_{max}, Fig 4C) and relaxation (dP/dt_{min},Fig 4D). All other hemodynamic measurements are shown in Supplemental Table 1.

$_{m}Ca^{2+}$ signaling modulates energetics by activating Ca^{2+}-dependent dehydrogenases, as well as possible direct action on ETC components[32,33,34]. We have previously reported that mtCU mediated Ca^{2+} uptake stimulates mitochondrial energetics and is necessary for increased contractility during adrenergic stimulation[5]. To examine if mitochondrial energetics were altered with MCUB expression we isolated ACMs from MCM and MCUB-Tg x MCM mice and examined oxidative phosphorylation by monitoring oxygen consumption rates (OCR) (Fig 4E). MCUB expression significantly decreased maximal respiration and spare respiratory capacity, yet had no effect on basal respiration, ATP-linked respiration, or proton leak (Fig 4F). Next, we performed Western blots to assess phosphorylation at S293 of pyruvate dehydrogenase (p-PDH), the inhibitory phosphorylation site that is dephosphorylated by the $_{m}Ca^{2+}$-dependent pyruvate dehydrogenase phosphatase. Densitometry revealed that MCUB gain-of-function increased baseline p-PDH ~2.3 fold (corrected to total PDH-E1α), as compared to ventricular samples isolated from MCM control hearts (Fig 4G). There was no difference in total PDH-E1α between groups (Supp. Fig 4A). We also evaluated p-PDH in cardiac lysates from hearts subjected to iso infusion and found that MCUB expression significantly blocked dephosphorylation indicating an inability to increase PDH activity (Fig 4H). There was no difference in total PDH-E1α between groups (Supp. Fig 4B). These results suggest that MCUB inhibition of $_{m}Ca^{2+}$ uptake is a powerful mechanism to downregulate mitochondrial bioenergetics by inactivating PDH and diminishing oxidative capacity during stress and that this mechanism may be sufficient to impair contractile reserve. Surprisingly, the effect of MCUB on LV function was even greater than what we reported with cardiomyocyte-specific deletion of *Mcu*[5]. We hypothesize that this may be largely dependent upon the temporal inhibition of mtCU flux as Cre-activation of transgene expression is rapid in this model (<24h), whereas deletion of *Mcu* occurs over days to weeks due to the slow protein turnover rate. This finding may also shed light on other reports where a mild-phenotype was observed with germline or chronic modulation of *Mcu*[9,35] and suggests alternative energetic pathways are quickly activated in response to impaired $_{m}Ca^{2+}$ uptake.

One month following MCUB induction cellular bioenergetics and contractile reserve are restored

It was unclear how the acute cardiac dysfunction of the MCUB transgenic mouse was completely reversed one month following expression, especially because cardiac mitochondria from MCUB-Tg mice still displayed reduced $_{m}Ca^{2+}$ uptake as exhibited by their resistance to mitochondrial swelling (Fig 3E–G, Supp. Fig 3L–N). To determine the mechanism accounting for the compensated phenotype, we first evaluated the protein expression of MCUB and MCU in cardiac protein lysates of MCM and MCUB-Tg x MCM mice one month following tamoxifen administration. We found MCUB was still upregulated to a similar extent as that seen with acute expression (Fig 5A–C). We next examined the phosphorylation status of pyruvate dehydrogenase and found it was no different between chronic MCUB expression and controls, indicating a restoration in PDH activity (Fig 5D–E). Next, we assessed oxidative phosphorylation and found that MCUB-Tg x MCM ACMs had restored OCR indices to that of controls (Fig 5 F–G) further indicating a restoration of cellular bioenergetics. Last, we assessed cardiac contractility using invasive hemodynamics and found that adrenergic-driven contractility (dP/dt maximum, Fig 5I) and relaxation (dP/dt

minimum, Fig 5J) of MCUB-Tg x MCM mice had returned to MCM control levels. Given the divergent post-IR phenotype of our MCUB mutant mouse (acute expression resulted in lethality during ischemia while 1m post-gene induction was cardioprotective) we hypothesize that acute expression of MCUB impaired mitochondrial energetics. We suspect that ATP supply was insufficient during the high-stress/demand of acute IR-injury and that calcium-independent compensatory mechanisms are activated during sustained MCUB expression (1m) to restore bioenergetics and cardiac function. These compensatory energetic mechanisms are sufficient to now make dampening $_{m}Ca^{2+}$ uptake more favorable and reduce $_{m}Ca^{2+}$ overload and cell death.

MCUB expression displaces MCU-subunits in the mtCU to modulate MICU1/2 gating

To determine the mechanism whereby MCUB regulates mtCU function we examined the functional/high-MW channel in mitochondria isolated from the hearts of our mutant MCUB expression model. MCM and MCUB-Tg x MCM were injected with tamox for four consecutive days and on day five mitochondria were isolated and fractionated by size-exclusion FPLC. Fractions ranging from ~200–900 kD were run under reducing conditions and immunoblotted to evaluate the molecular composition of the mtCU (Fig 6A–6D). We first examined MCUB expression and noted that MCUB was absent from the mtCU in control hearts. In contrast, mitochondria isolated from our overexpression model (MCUB-Tg x MCM) displayed clear expression of MCUB in the high-MW fractions similar to that observed 24h after IR-injury (Fig 6A). Next, we immunoblotted for the pore-component, MCU, and found that MCUB expression decreased the overall size of the mtCU, indicated by a rightward shift in the chromatograph (Fig 6B). To ascertain if MCUB expression impacted the association of other mtCU components we examined the mtCU regulators MICU1 and MICU2. Incorporation of MCUB into the mtCU markedly reduced both MICU1 and MICU2 expression in the high-MW complex (Fig 6C, 6D). Given the impact of MCUB expression on MICU1/2 association with the mtCU we next sought to determine if MICUs directly interact with MCUB. Employing c-terminal tags we co-expressed MCUB-HA with MCU-FLAG, MICU1-FLAG, or MICU2-FLAG. 48h after transfection we immunoprecipitated (IP'd) under stringent conditions to assess direct binding with an HA antibody (MCUB) and immunoblotted for FLAG (Fig 6E). MCUB directly interacted with MCU, but pull-downs with MCUB resulted in no detection of MICU1 or MICU2 immunoreactivity. MCUB expression was similar among all experimental groups (IB:HA, Fig 6E). To validate this result we next performed reverse IPs and co-expressed MICU1-FLAG or MICU2-FLAG (Fig 6F, 6G) with MCU-HA or MCUB-HA. IPs of MICU1 and MICU2 both showed clear interaction with MCU, but no binding of MCUB (Fig 6F, 6G). FLAG expression (MICU1-FLAG or MICU2-FLAG) was similar in all groups (Fig 6F, 6G). We further confirmed this by performing endogenous IPs for MCUB in MCUB-Tg x MCM cardiac protein lysates (Supp. Figure 5A). We confirmed MCUB interacted with MCU (Supp. Figure 5B), but did not interact with MICU1 (Supp. Fig 5C). We next examined if MCUB could interact with EMRE independent of MCU by performing co-transfections of EMRE-FLAG with either MCU-HA or MCUB-HA in a *MCU*$^{-/-}$ HeLa cell line (Supp. Fig 5G). MCU and MCUB both interacted with EMRE. To further validate the FPLC results we extracted native complexes from cardiac mitochondrial samples for blue native PAGE analysis of the mtCU (Supp. Fig 5D–F). Densitometric analysis of MICU1 immunoblots

indicated expression was significantly reduced in high-MW native complexes from MCUB-Tg x MCM hearts compared to MCM controls after correcting to total mitochondrial protein (Supp. Fig 5D–E). Densitometric analysis of MCU immunoblots of controls indicated increased MCU expression in higher MW complexes as compared to MCUB-Tg x MCM hearts (Supp. Fig 5F). All full-length Western blots for all data are presented in Supp. Figures 6–9.

In summary, these results suggest that MCUB displaces MCU from the mtCU and thereby indirectly modulates the association of MICUs with the functional channel (i.e. MICU1/2 only bind MCU not MCUB and thereby are displaced upon MCUB expression in the functional uniporter complex). Our results suggest that the expression of MCUB is a mechanism to decrease mtCU uptake by modulating the molecular composition of the mtCU.

Discussion

Here we identified a new molecular mechanism regulating the mitochondrial calcium uniporter (mtCU). We discovered that MCUB is a powerful regulator of mitochondrial calcium uptake by modulating the incorporation of channel subunits and therein modifies the stoichiometry and function of the uniporter. In addition, our study reveals that MCUB is upregulated following acute cardiac injury and that this is likely a compensatory mechanism to lessen mitochondrial calcium overload during stress. We also provide data suggesting that increased MCUB incorporation into the mtCU does come at a cost, as MCUB-mediated downregulation of mtCU function impairs mitochondrial energetics during stress.

Raffaello et al. discovered the *MCU* paralog, *MCUB*, and in agreement with our study showed that siRNA silencing of MCUB increased $_{m}Ca^{2+}$ transients. The Rizzuto led group also reported that expressing *MCUB* alone in a lipid bilayer alone did not result in a channel with Ca^{2+} conductance[21], in contrast to what was reported for the pore-forming subunit, MCU[36, 37]. This led to the conclusion that this paralog exists as a dominant negative regulator of channel function and perhaps primarily impacted calcium permeation or pore function. While this founding discovery presents strong evidence that MCUB is a component of the mtCU many questions remained. How does MCUB regulate the mtCU? Is it a physiological regulator of mitochondrial calcium uptake? How does its association with the uniporter impact cellular function?

Employing size-exclusion chromatography we examined how mtCU stoichiometry changed with loss or expression of *MCUB*. We deleted MCUB in HeLa cells because of their relatively high level of MCUB expression and vast historical data with regards to the molecular regulation of the mtCU to allow for comparisons with previously published studies. Loss of MCUB enriched the levels of MCU, MICU1, and MICU2 in the high-MW mtCU (the physiological/functional uniporter). Conversely, cardiomyocyte-specific overexpression of MCUB in the heart decreased the overall size of the mtCU (rightward shift in the MCU chromatogram) and decreased both MICU1 and MICU2 association with the high-MW complex. These data suggest that MCUB may regulate the uniporter by altering the subunits that are present in the functional complex and suggests an alternative

mechanism of regulation differing to, or beyond, altering the structure of the pore. Since we found that MCUB was not present in the uniporter complex at baseline but was incorporated into the channel after cardiac injury it is likely that this is a stress-responsive mechanism in the heart to limit $_{m}Ca^{2+}$ overload. It is possible that this may also be a mechanism to mediate differences in uptake between different cell types, as MCUB expression is reported to be tissue dependent[21].

MCUB gain- or loss-of-function significantly altered the biophysical properties of $_{m}Ca^{2+}$ uptake mostly at higher cytosolic calcium load. Mitoplast patch clamping studies indicated increased channel capacitance with MCUB deletion, which we attribute to either an overall increase in mtCU density (# of uniporters per mitochondrion) or alteration in mtCU gating/activation. By incrementally changing the extra-mitochondrial Ca^{2+} load we could resolve an increase in $_{m}Ca^{2+}$ uptake that was most apparent at concentrations >3μM. Given these changes we hypothesize that increasing MCUB expression displaces MCU subunits from the mtCU and thus is indirectly altering the association of MICU1/2 with the uniporter. This rationale is supported by our data showing that MICU1 and MICU2 can bind MCU, but do not directly interact with MCUB. This mechanism could explain the decrease in uptake at higher calcium levels, as MICU1/2 are reported to be necessary for cooperative activation of the mtCU[12, 13, 16, 38].

Acute increases in cardiomyocyte MCUB expression had a profound effect on cardiac physiology. We found that mitochondrial bioenergetics were severely impaired following the induction of MCUB expression. As we previously reported, the likely mechanism driving this impairment was an inability to activate the calcium-dependent dehydrogenases, notably pyruvate dehydrogenase (PDH). This in turn severely limited oxidative capacity decreasing both maximal respiration and reserve capacity. Further, this loss of energetic capacity manifested in MCUB overexpressing mice failing to increase cardiac function in response to β-adrenergic stimulation. This lack of energetic responsiveness was most apparent when mice with acute expression of MCUB (within 1w of tamox administration) were subjected to myocardial IR-injury which resulted in nearly all mice dying within minutes of LCA ligation (ischemic period). This is in stark contrast to MCUB overexpressing mice that were allowed to rest for 1m after tamoxifen treatment when cardiac dysfunction is no longer present. With this protocol we found that MCUB overexpression reduced infarct size by ~50% with a noted decrease in mitochondrial swelling, indicative of reduced mPTP activation. We've previously reported a nearly identical phenotype with deletion of MCU, bolstering the notion that mitochondrial-calcium overload is a major contributor to IR-induced cardiomyocyte death[5]. We suspect that these divergent phenotypes are due to compensatory changes that occur following increased MCUB expression. A few possibilities exist that may account for this difference. Compensatory changes such as the upregulation of cardioprotective signaling or activation of alternative energetic pathways may contribute. We noted a full restoration of cellular bioenergetics one month after MCUB induction, including the restoration of PDH activity. This compensation did not appear to be calcium-dependent as chronic expression of MCUB was still associated with a significant reduction in calcium-induced mitochondrial swelling. This suggests alternative mechanisms may be responsible. PDH phosphatase is regulated by Ca^{2+} and Mg^{2+}, while PDH kinase is allosterically inhibited by ADP, NAD+, coenzyme A, and pyruvate; and activated by ATP, NADH, and

acetyl-CoA. It is likely that allosteric regulation independent of calcium is compensating in our mutant mouse model, although further investigation is warranted.

It should be noted that this model might help explain conflicting reports in various *Mcu* knockout models, which have shown divergent outcomes with regards to IR-injury. Germline deletion of MCU resulted in no change in infarct size[9], whereas conditional deletion in the adult heart reduced infarct size following IR-injury[5, 6]. Here we show that temporal compensatory mechanisms can account for a very dramatic difference in phenotype in the same mutant mouse and suggest that carefully planned experiments are needed to avoid misinterpretation of results with regards to the genetic perturbation of mitochondrial calcium exchange. Additionally, we were very surprised to see that our MCUB transgenic mouse developed acute cardiac dysfunction 1 wk post MCUB induction, as our MCU cKO mouse did not display any baseline cardiac phenotype[5]. This is surprising because MCU deletion and MCUB overexpression have a similar functional outcome of blocking or inhibiting acute $_{m}Ca^{2+}$ uptake. This differential phenotype is likely due to the time it takes to block $_{m}Ca^{2+}$ uptake. Upregulation of MCUB likely takes place rapidly, within hours, while complete loss of MCU with Cre-mediated deletion requires turnover of the existing protein, half-life upwards of 72 hours. This difference in time to complete inhibition of mitochondrial calcium uptake may allow compensatory mechanisms to be activated resulting in divergent cellular physiology. This adds further complexity into interpreting results acquired from different mtCU genetic mouse models and protocols.

Conclusions:

In this study, we report a new mechanism to regulate mtCU function and mitochondrial calcium uptake. Our findings advocate that the assembly and stoichiometry of the subunits comprising the uniporter is critical to its function and that MCUB is a prominent regulator of uniporter composition. This suggests that the evaluation of the subunits comprising the functional, high-mw complex is an important experimental consideration and suggests that post-translational regulation of the mtCU is a critical mechanism to modulate channel gating to fine-tune $_{m}Ca^{2+}$ uptake and modulate mitochondrial bioenergetics during stress.

Supplementary Material

Refer to Web version on PubMed Central for supplementary material.

Acknowledgments:

The authors would like to express thanks to Dr. Rajika Roy for technical assistance and Trevor Tierney for scientific and administrative assistance.

Sources of Funding:

NIH to J.W.E.: R01HL142271, R01HL136954, R01HL123966, P01HL134608-sub-5483; American Heart Association to D.T.: 17POST33660251; American Heart Association to T.S.L.: 15PRE25080299; American Heart Association to J.P.L.: 17PRE33460423

Non-standard abbreviations and Acronyms:

AAR	area-at-risk
AAV	adeno-associated virus
ACMs	adult cardiomyocytes
CV-Sα	Complex V; F_1F_O ATP synthase
Ca^{2+}	calcium
CAT	chloramphenicol acetyltransferase
$_cCa^{2+}$	cytosolic Ca^{2+}
dP/dt_{max}	contractility
dP/dt_{min}	relaxation
IP'd	immunoprecipitated
ER	endoplasmic reticulum
ETC	electron transport chain
EMRE	essential MCU regulator
FPLC	fast protein liquid chromatography
IMM	inner mitochondrial membrane
IP3R	inositol 1,4,5-triphosphate receptor
IR	ischemia-reperfusion injury
Iso	isoproterenol
LCA	left coronary artery
$_mCa^{2+}$	mitochondrial calcium
MCM	αMHC Mer-Cre-Mer mutant mouse
mCRC	mitochondrial calcium retention capacity
MCU	mitochondrial calcium uniporter
$MCUB^{-/-}$	stable *MCUB* knockout HeLa cell line
MCU cKO	MCU conditional knockout mouse model
MCUR1	mitochondrial calcium uniporter regulator 1
MI	myocardial infarction
MICU1	Mitochondrial Calcium Uptake 1

MICU2	Mitochondrial Calcium Uptake 2
MPTP	mitochondrial permeability transition pore
mtCU	mitochondrial calcium uniporter channel complex
MW	molecular weight
OCR	oxygen consumption rate
p-PDH	phosphorylation of Pyruvate Dehydrogenase-e1α subunit at Ser-293
PDH	Pyruvate Dehydrogenase
tamox	tamoxifen
WT	wild-type
Δψ	mitochondrial membrane potential

References

1. Baughman JM, Perocchi F, Girgis HS, Plovanich M, Belcher-Timme CA, Sancak Y, Bao XR, Strittmatter L, Goldberger O, Bogorad RL, Koteliansky V and Mootha VK. Integrative genomics identifies MCU as an essential component of the mitochondrial calcium uniporter. Nature. 2011;476:341–345. [PubMed: 21685886]
2. Kirichok Y, Krapivinsky G and Clapham DE. The mitochondrial calcium uniporter is a highly selective ion channel. Nature. 2004;427:360–364. [PubMed: 14737170]
3. De Stefani D, Raffaello A, Teardo E, Szabo I and Rizzuto R. A forty-kilodalton protein of the inner membrane is the mitochondrial calcium uniporter. Nature. 2011;476:336–340. [PubMed: 21685888]
4. Bernardi P Modulation of the mitochondrial cyclosporin A-sensitive permeability transition pore by the proton electrochemical gradient. Evidence that the pore can be opened by membrane depolarization. J Biol Chem. 1992;267:8834–8839. [PubMed: 1374381]
5. Luongo TS, Lambert JP, Yuan A, Zhang X, Gross P, Song J, Shanmughapriya S, Gao E, Jain M, Houser SR, Koch WJ, Cheung JY, Madesh M and Elrod JW. The Mitochondrial Calcium Uniporter Matches Energetic Supply with Cardiac Workload during Stress and Modulates Permeability Transition. Cell reports. 2015;12:23–34. [PubMed: 26119731]
6. Kwong JQ, Lu X, Correll RN, Schwanekamp JA, Vagnozzi RJ, Sargent MA, York AJ, Zhang J, Bers DM and Molkentin JD. The Mitochondrial Calcium Uniporter Selectively Matches Metabolic Output to Acute Contractile Stress in the Heart. Cell reports. 2015;12:15–22. [PubMed: 26119742]
7. Luongo TS, Lambert JP, Gross P, Nwokedi M, Lombardi AA, Shanmughapriya S, Carpenter AC, Kolmetzky D, Gao E, van Berlo JH, Tsai EJ, Molkentin JD, Chen X, Madesh M, Houser SR and Elrod JW. The mitochondrial Na(+)/Ca(2+) exchanger is essential for Ca(2+) homeostasis and viability. Nature. 2017;545:93–97. [PubMed: 28445457]
8. Vasington FD, Gazzotti P, Tiozzo R and Carafoli E. The effect of ruthenium red on Ca2+ transport and respiration in rat liver mitochondria. Biochimica et Biophysica Acta (BBA) - Bioenergetics. 1972;256:43–54. [PubMed: 4257941]
9. Pan X, Liu J, Nguyen T, Liu C, Sun J, Teng Y, Fergusson MM, Rovira II, Allen M, Springer DA, Aponte AM, Gucek M, Balaban RS, Murphy E and Finkel T. The physiological role of mitochondrial calcium revealed by mice lacking the mitochondrial calcium uniporter. Nat Cell Biol. 2013;15:1464–1472. [PubMed: 24212091]
10. Oxenoid K, Dong Y, Cao C, Cui T, Sancak Y, Markhard AL, Grabarek Z, Kong L, Liu Z, Ouyang B, Cong Y, Mootha VK and Chou JJ. Architecture of the mitochondrial calcium uniporter. Nature. 2016;533:269–273. [PubMed: 27135929]

11. Perocchi F, Gohil VM, Girgis HS, Bao XR, McCombs JE, Palmer AE and Mootha VK. MICU1 encodes a mitochondrial EF hand protein required for Ca(2+) uptake. Nature. 2010;467:291–296. [PubMed: 20693986]
12. Paillard M, Csordas G, Szanda G, Golenar T, Debattisti V, Bartok A, Wang N, Moffat C, Seifert EL, Spat A and Hajnoczky G. Tissue-Specific Mitochondrial Decoding of Cytoplasmic Ca(2+) Signals Is Controlled by the Stoichiometry of MICU1/2 and MCU. Cell reports. 2017;18:2291–2300. [PubMed: 28273446]
13. Csordas G, Golenar T, Seifert EL, Kamer KJ, Sancak Y, Perocchi F, Moffat C, Weaver D, de la Fuente Perez S, Bogorad R, Koteliansky V, Adijanto J, Mootha VKand Hajnoczky G. MICU1 controls both the threshold and cooperative activation of the mitochondrial Ca(2)(+) uniporter. Cell Metab. 2013;17:976–987. [PubMed: 23747253]
14. Mallilankaraman K, Doonan P, Cardenas C, Chandramoorthy HC, Muller M, Miller R, Hoffman NE, Gandhirajan RK, Molgo J, Birnbaum MJ, Rothberg BS, Mak DO, Foskett JK and Madesh M. MICU1 is an essential gatekeeper for MCU-mediated mitochondrial Ca(2+) uptake that regulates cell survival. Cell. 2012;151:630–644. [PubMed: 23101630]
15. Liu JC, Liu J, Holmstrom KM, Menazza S, Parks RJ, Fergusson MM, Yu ZX, Springer DA, Halsey C, Liu C, Murphy E and Finkel T. MICU1 Serves as a Molecular Gatekeeper to Prevent In Vivo Mitochondrial Calcium Overload. Cell reports. 2016;16:1561–1573. [PubMed: 27477272]
16. Payne R, Hoff H, Roskowski A and Foskett JK. MICU2 Restricts Spatial Crosstalk between InsP3R and MCU Channels by Regulating Threshold and Gain of MICU1-Mediated Inhibition and Activation of MCU. Cell reports. 2017;21:3141–3154. [PubMed: 29241542]
17. Plovanich M, Bogorad RL, Sancak Y, Kamer KJ, Strittmatter L, Li AA, Girgis HS, Kuchimanchi S, De Groot J, Speciner L, Taneja N, Oshea J, Koteliansky V and Mootha VK. MICU2, a paralog of MICU1, resides within the mitochondrial uniporter complex to regulate calcium handling. PloS one. 2013;8:e55785. [PubMed: 23409044]
18. Sancak Y, Markhard AL, Kitami T, Kovacs-Bogdan E, Kamer KJ, Udeshi ND, Carr SA, Chaudhuri D, Clapham DE, Li AA, Calvo SE, Goldberger O and Mootha VK. EMRE is an essential component of the mitochondrial calcium uniporter complex. Science (New York, NY). 2013;342:1379–1382.
19. Vais H, Mallilankaraman K, Mak DD, Hoff H, Payne R, Tanis JE and Foskett JK. EMRE Is a Matrix Ca(2+) Sensor that Governs Gatekeeping of the Mitochondrial Ca(2+) Uniporter. Cell reports. 2016;14:403–410. [PubMed: 26774479]
20. Tomar D, Dong Z, Shanmughapriya S, Koch DA, Thomas T, Hoffman NE, Timbalia SA, Goldman SJ, Breves SL, Corbally DP, Nemani N, Fairweather JP, Cutri AR, Zhang X, Song J, Jana F, Huang J, Barrero C, Rabinowitz JE, Luongo TS, Schumacher SM, Rockman ME, Dietrich A, Merali S, Caplan J, Stathopulos P, Ahima RS, Cheung JY, Houser SR, Koch WJ, Patel V, Gohil VM, Elrod JW, Rajan S and Madesh M. MCUR1 Is a Scaffold Factor for the MCU Complex Function and Promotes Mitochondrial Bioenergetics. Cell reports. 2016;15:1673–1685. [PubMed: 27184846]
21. Raffaello A, De Stefani D, Sabbadin D, Teardo E, Merli G, Picard A, Checchetto V, Moro S, Szabo I and Rizzuto R. The mitochondrial calcium uniporter is a multimer that can include a dominant-negative pore-forming subunit. The EMBO journal. 2013;32:2362–2376. [PubMed: 23900286]
22. Ran FA, Hsu PD, Wright J, Agarwala V, Scott DA and Zhang F. Genome engineering using the CRISPR-Cas9 system. Nat Protoc. 2013;8:2281–2308. [PubMed: 24157548]
23. Zhou YY, Wang SQ, Zhu WZ, Chruscinski A, Kobilka BK, Ziman B, Wang S, Lakatta EG, Cheng H and Xiao RP. Culture and adenoviral infection of adult mouse cardiac myocytes: methods for cellular genetic physiology. Am J Physiol Heart Circ Physiol. 2000;279:H429–36. [PubMed: 10899083]
24. Frezza C, Cipolat S and Scorrano L. Organelle isolation: functional mitochondria from mouse liver, muscle and cultured fibroblasts. Nat Protoc. 2007;2:287–295. [PubMed: 17406588]
25. Elrod JW, Wong R, Mishra S, Vagnozzi RJ, Sakthievel B, Goonasekera SA, Karch J, Gabel S, Farber J, Force T, Brown JH, Murphy E and Molkentin JD. Cyclophilin D controls mitochondrial pore-dependent Ca(2+) exchange, metabolic flexibility, and propensity for heart failure in mice. J Clin Invest. 2010;120:3680–3687. [PubMed: 20890047]
26. Kirichok Y, Krapivinsky G and Clapham DE. The mitochondrial calcium uniporter is a highly selective ion channel. Nature. 2004;427:360. [PubMed: 14737170]

27. Gao E, Lei YH, Shang X, Huang ZM, Zuo L, Boucher M, Fan Q, Chuprun JK, Ma XL and Koch WJ. A novel and efficient model of coronary artery ligation and myocardial infarction in the mouse. Circ Res. 2010;107:1445–1453. [PubMed: 20966393]

28. Zhao Y, Araki S, Wu J, Teramoto T, Chang Y-F, Nakano M, Abdelfattah AS, Fujiwara M, Ishihara T, Nagai T and Campbell RE. An expanded palette of genetically encoded Ca^{2+} indicators. Science (New York, NY). 2011;333:1888–1891.

29. Bers DM, Despa S and Bossuyt J. Regulation of Ca2+ and Na+ in normal and failing cardiac myocytes. Ann NY Acad Sci. 2006;1080:165–177. [PubMed: 17132783]

30. Sohal DS, Nghiem M, Crackower MA, Witt SA, Kimball TR, Tymitz KM, Penninger JM and Molkentin JD. Temporally regulated and tissue-specific gene manipulations in the adult and embryonic heart using a tamoxifen-inducible Cre protein. Circ Res. 2001;89:20–25. [PubMed: 11440973]

31. Joiner M-lA, Koval OM, Li J, He BJ, Allamargot C, Gao Z, Luczak ED, Hall DD, Fink BD, Chen B, Yang J, Moore SA, Scholz TD, Strack S, Mohler PJ, Sivitz WI, Song L-Sand Anderson ME. CaMKII determines mitochondrial stress responses in heart. Nature. 2012;491:269. [PubMed: 23051746]

32. Denton RM, McCormack JG and Edgell NJ. Role of calcium ions in the regulation of intramitochondrial metabolism. Effects of Na+, Mg2+ and ruthenium red on the Ca2+-stimulated oxidation of oxoglutarate and on pyruvate dehydrogenase activity in intact rat heart mitochondria. Biochem J. 1980;190:107–117. [PubMed: 6160850]

33. Glancy B and Balaban RS. Role of Mitochondrial Ca2+ in the Regulation of Cellular Energetics. Biochemistry. 2012;51:2959–2973. [PubMed: 22443365]

34. Denton RM, Randle PJ and Martin BR. Stimulation by calcium ions of pyruvate dehydrogenase phosphate phosphatase. Biochem J. 1972;128:161–163. [PubMed: 4343661]

35. Rasmussen TP, Wu Y, Joiner ML, Koval OM, Wilson NR, Luczak ED, Wang Q, Chen B, Gao Z, Zhu Z, Wagner BA, Soto J, McCormick ML, Kutschke W, Weiss RM, Yu L, Boudreau RL, Abel ED, Zhan F, Spitz DR, Buettner GR, Song LS, Zingman LV and Anderson ME. Inhibition of MCU forces extramitochondrial adaptations governing physiological and pathological stress responses in heart. Proc Nat Acad Sci USA. 2015;112:9129–9134. [PubMed: 26153425]

36. Chaudhuri D, Sancak Y, Mootha VK and Clapham DE. MCU encodes the pore conducting mitochondrial calcium currents. eLife. 2013;2:e00704. [PubMed: 23755363]

37. De Stefani D, Raffaello A, Teardo E, Szabò I and Rizzuto R. A forty-kilodalton protein of the inner membrane is the mitochondrial calcium uniporter. Nature. 2011;476:336. [PubMed: 21685888]

38. Patron M, Checchetto V, Raffaello A, Teardo E, Vecellio Reane D, Mantoan M, Granatiero V, Szabo I, De Stefani D and Rizzuto R. MICU1 and MICU2 finely tune the mitochondrial Ca2+ uniporter by exerting opposite effects on MCU activity. Molecular cell. 2014;53:726–737. [PubMed: 24560927]

Clinical Perspective:

What is new?

- MCUB is absent from the uniporter complex (mtCU) in the homeostatic heart (cardiomyocytes) but is incorporated into the mtCU following ischemia injury representing an endogenous mechanism to limit mitochondrial calcium overload during stress.
- MCUB negatively regulates $_{m}Ca^{2+}$ uptake by altering the macromolecular assembly and stoichiometry of mtCU subunits through displacement of MCU-MICU1 defining a new molecular mechanism to fine-tune mitochondrial calcium uptake.
- The increased incorporation of MCUB into the mtCU is too little and too late to limit acute cell death following IR injury but may limit cell loss during chronic stress.

What are the clinical implications?

- MCUB represents a novel therapeutic target to modulate $_{m}Ca^{2+}$ uptake in disease states featuring $_{m}Ca^{2+}$ overload, such as myocardial infarction and heart failure.

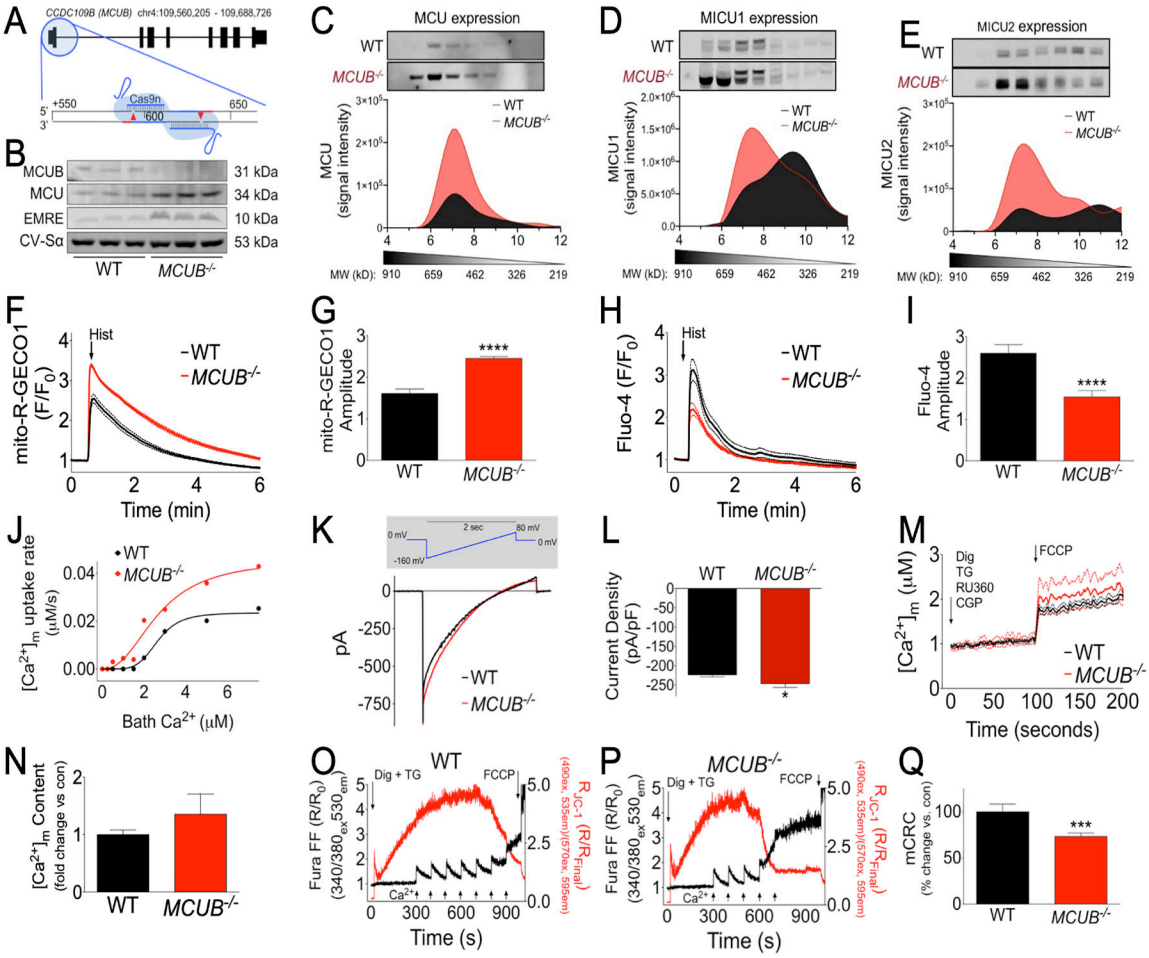

Figure 1. *MCUB* deletion alters mtCU stoichiometry, and function.

A) Cas9n was targeted to exon 1 of *MCUB*. Clonal lines were evaluated after puromycin selection. **B)** Western blots for MCUB, MCU, and EMRE, in wild-type (WT) vs *MCUB*$^{-/-}$ cell lines. Complex-V Sα was used as a mitochondrial loading control; n=3 for both groups. **C-E)** WT and *MCUB*$^{-/-}$ cells were fractionated by size-exclusion FPLC and fractions were immunoblotted under reducing conditions. Densitometry was performed to generate chromatographs of relative expression for mtCU subunits: **C)** MCU **D)** MICU1 **E)** MICU2. **F)** WT and *MCUB*$^{-/-}$ cells were transduced with AAV6-mito-R-GECO1 and fluorescence was recorded to monitor $_{m}Ca^{2+}$ dynamics following histamine stimulation. **G)** Amplitude of $_{m}Ca^{2+}$ transients (peak intensity – baseline (F/F_0)-F_0); n=32 cells for WT, n=33 cells for *MCUB*$^{-/-}$. **H)** $_{C}Ca^{2+}$ (Fluo4-AM) recordings following histamine stimulation. **I)** Amplitude of $_{c}Ca^{2+}$ transients (peak intensity – baseline (F/F_0)-F_0); n=37 cells for WT, n=41 cells for *MCUB*$^{-/-}$. **J)** Ratiometric monitoring of bath $[Ca^{2+}]$ levels (Fura-FF) and $\Delta\Psi$ (JC-1) following permeabilization. Bath Ca^{2+} ranged from 0.5 – 7.5 μM; representative experiment from n=3. **K)** Mitoplasts from WT and *MCUB*$^{-/-}$ cells were patch clamped to record MCU current (I_{MCU}) in picoamperes; pA). **L)** Current density (picoamperes/picofarad; pA/pF); n=8 for WT, n=7 for *MCUB*$^{-/-}$. **M)** Fura-2 recording of mitochondrial free-Ca^{2+} content in matrix. **N)** Fold change in mitochondrial free-$[Ca^{2+}]$ content in *MCUB*$^{-/-}$ cells vs WT; n=7

for WT, n=6 for *MCUB*$^{-/-}$. **O)** Mitochondrial calcium retention capacity (mCRC) recording in WT and **P)** *MCUB*$^{-/-}$ cells during repetitive additions of 10-μM Ca^{2+} (black arrows) until membrane potential collapse; representative transients from n=4 experiments. **Q)** Percent change in mCRC, *MCUB*$^{-/-}$ vs. WT; n=4 per group. *Calcium traces: solid line = mean, dashed line = SEM. All data are shown as mean +/− SEM. ****p<0.0001, *** p<0.001, *p<0.05.*

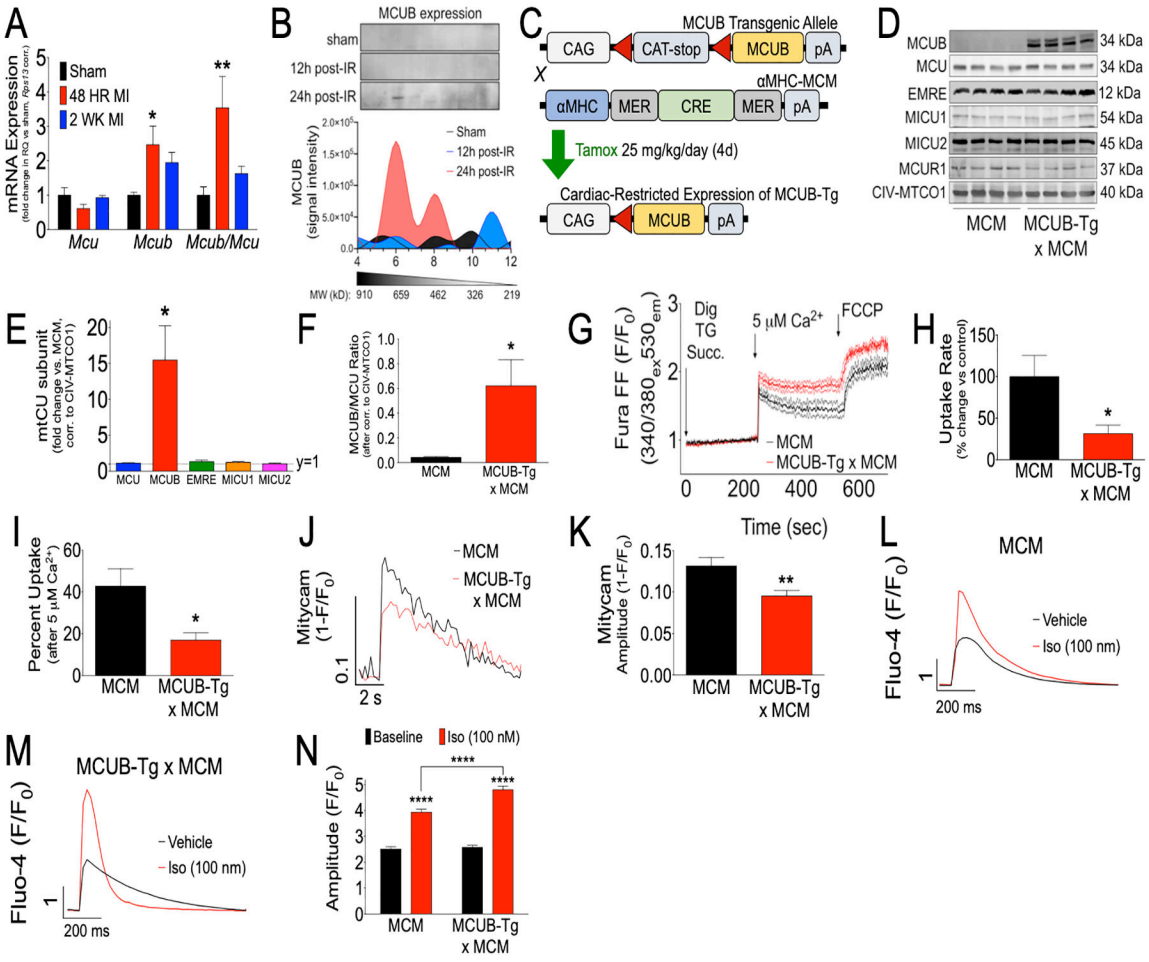

Figure 2. MCUB incorporates into the mtCU complex after injury, compelling the generation of a MCUB conditional mutant mouse model.

A) *Mcu*, *Mcub*, and the *Mcub/Mcu* mRNA expression in cardiac tissue of mice subjected to sham, 48h myocardial infarction (MI), and 2w MI; n=3–4 mice per group. **B)** Relative expression of MCUB in the high-MW mtCU from cardiac mitochondria of mice subjected to a sham procedure, 40 min ischemia 12h reperfusion (12h post-IR), or 24h reperfusion (24h post-IR); n=4 mice per group. **C)** *MCUB* conditional gain-of-function mice (MCUB-Tg) were generated using a flox-stop strategy. **D)** Immunoblots of mtCU components from cardiac lysates of MCM and MCUB-Tg x MCM 1d following tamoxifen administration. Complex IV-MTCO1 was used as a loading control. **E)** Fold change of indicated mtCU subunit vs. MCM control after correcting to CIV-MTCO1; n=4 mice per group. **F)** MCUB/MCU cardiac protein ratio. **G-I)** Ratiometric monitoring of bath [Ca^{2+}] levels (Fura-FF) in permeabilized MCM and MCUB-Tg x MCM cardiomyocytes following a 5 μM Ca^{2+} bolus; n=3 mice per group. **H)** Percent change in [$_mCa^{2+}$] uptake rate. **I)** Percent change in total [$_mCa^{2+}$] $^+$ uptake. **J)** $_mCa^{2+}$ transients (Mitycam) in cardiomyocytes paced at 0.1 Hz. **K)** Amplitude of $_mCa^{2+}$ transients ($1-F/F_0$); n=23 cells for MCM, n=30 cells for MCUB-Tg x MCM. **L-M)** $_cCa^{2+}$ transients (Fluo4-AM) in **L)** MCM and **M)** MCUB-Tg x MCM cardiomyocytes paced at 1 Hz, treated with vehicle (Veh) or Isoproterenol (Iso). **N)** Amplitude of $_cCa^{2+}$ transients (F/F_0); n=51 cells for MCM, n=56 cells for MCM plus iso,

n=61 cells for MCUB-Tg x MCM, n=57 cells for MCUB-Tg x MCM plus iso. *Data are shown as mean +/− SEM. ****p<0.0001, **p<0.01, *p<0.05*.

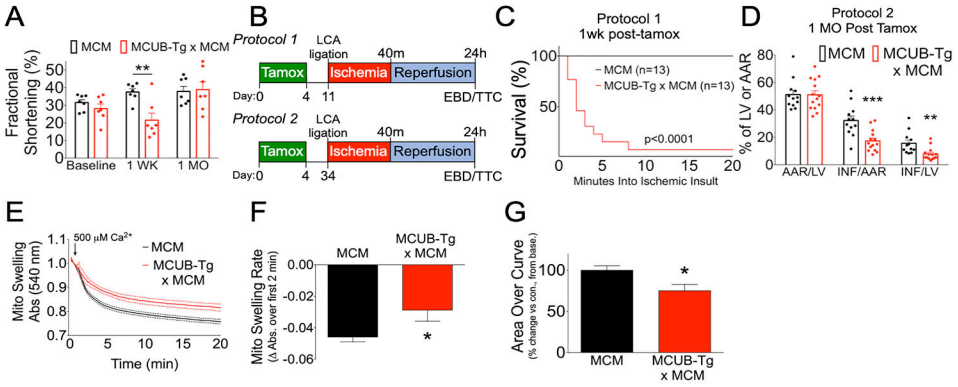

Figure 3. Cardiomyocyte overexpression of MCUB induces a transient cardiac phenotype and differential response to IR-injury dependent upon length of time expressed.

A) Percent fractional shortening (%FS) at baseline, 1w following tamoxifen (tamox) injections, and 1m following tamox injections; n=7 per group. **B)** Tamox injected mice were subjected to 40 min of ischemia and 24h of reperfusion 1w (Protocol 1) and 1m (Protocol 2) after MCUB induction and area-at-risk (AAR) and infarct size (INF) were examined. **C)** Protocol 1: Kaplan-Meier survival curve of mice subjected to IR injury 1w after tamox; n=13 mice per group. **D)** Protocol 2: Assessment of AAR per left ventricle (AAR/LV), INF/AAR, and INF/LV; n=12 mice for MCM, n=14 mice for MCUB-Tg x MCM. **E)** Protocol 2: Mitochondrial swelling monitored after 500 μM bath Ca^{2+} injection, ventricular mitochondria isolated from MCM and MCUB-Tg x MCM hearts; n=3 mice per group. **F)** Rate of swelling (change in absorbance over first 2m) **G)** Percent change in swelling (area-over-the-curve). *All data are shown as mean +/− SEM. ***p<0.001, **p<0.01, *p<0.05.*

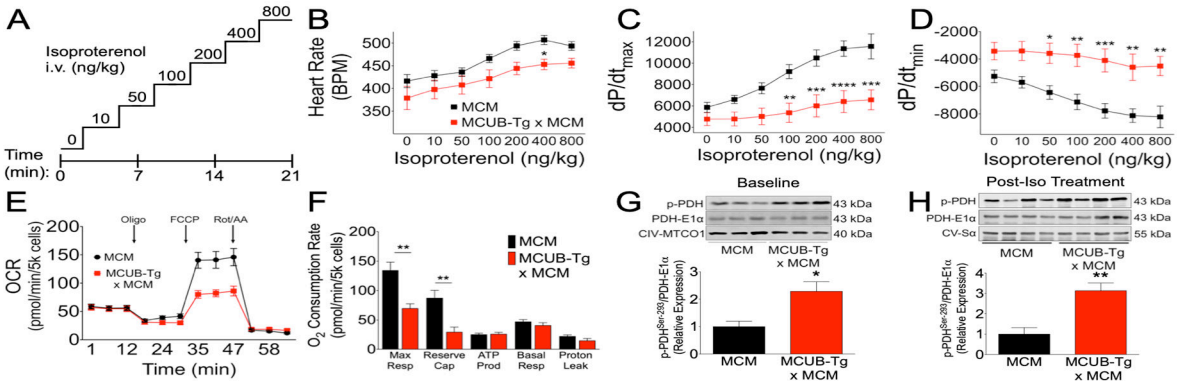

Figure 4. MCUB expression impairs mitochondrial energetics and LV contractility during stress.

A-D) MCM (n=11) and MCUB-Tg x MCM (n=6) mice received tamoxifen (tamox; 25 mg/kg/day) for 4d and 1d later were subjected to intravenous (i.v.) infusion of isoproterenol (Iso, 0–800 ng/kg) with invasive LV hemodynamic monitoring of: **B)** heart rate (beats/m), **C)** dP/dt maximum, and **D)** dP/dt minimum. **E)** 1d post-tamox adult cardiomyocytes were assayed for oxidative phosphorylation using a Seahorse bioanalyzer to measure the oxygen consumption rate (OCR); Oligo = oligomycin, FCCP = mitochondrial protonophore, Rot/AA = rotenone + antimycin A. **F)** Maximal respiration (FCCP-Rot/AA), reserve capacity (FCCP-base), ATP production (Oligo-base), baseline respiration, and proton leak (Oligo-Rot/AA) represented as picomoles O^2/min/5k cells; n=3 mice per group. **G)** Immunoblots for pyruvate dehydrogenase phosphorylation at $Serine^{293}$ (p-PDH), total Pyruvate Dehydrogenase E1-α (PDH-E1α), and the mitochondrial loading control Complex IV-MTCO1. Relative expression of p-PDH to PDH-E1α is depicted; n=3 per group. **H)** Cardiac protein lysates from post-Iso stressed hearts were immunoblotted for p-PDH, PDH-E1α, and Complex V-Sα; n=6 per group. Relative expression of P-PDH compared to total PDH-E1α is depicted. *All data are shown as mean +/− SEM. ****p<0.0001, ***p<0.001, **p<0.01, *p<0.05.*

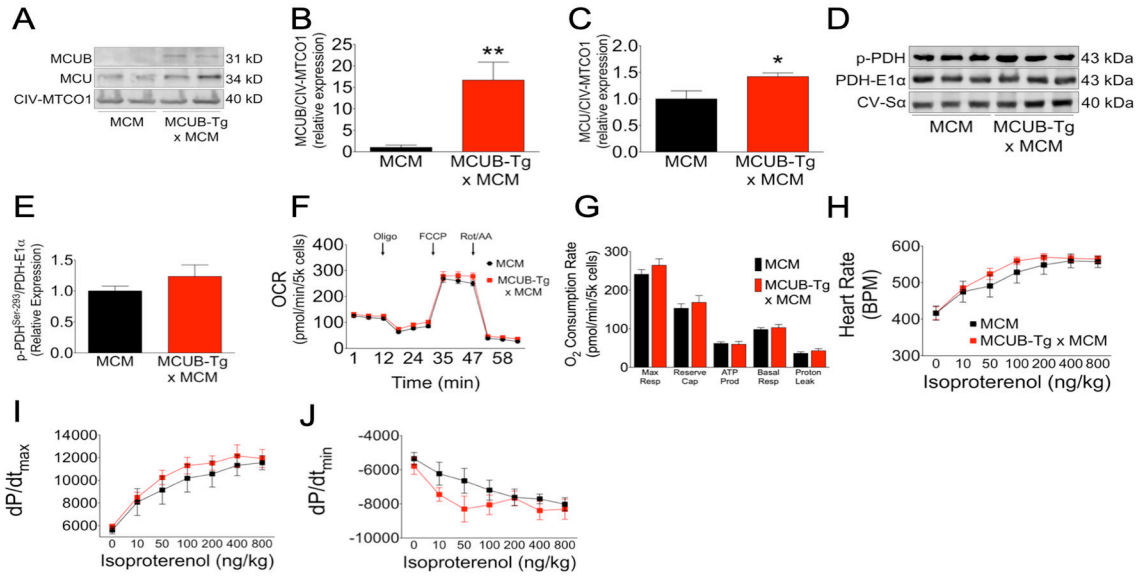

Figure 5. Compensatory restoration of cellular bioenergetics and contractile reserve in MCUB-Tg mice 1mo following tamox administration.

A-E) 1m after tamoxifen injection cardiac tissue of MCM and MCUB-Tg x MCM were immunoblotted for MCUB and MCU, Complex IV-MTCO1 was used as a loading control; n=4 mice per group. **B)** Relative expression of MCUB. **C)** Relative expression of MCU. **D)** Immunoblots for pyruvate dehydrogenase phosphorylation at Serine^{293} (p-PDH), total Pyruvate Dehydrogenase E1-α (PDH-E1α), and the mitochondrial loading control Complex V-Sα. **E)** Ratio of p-PDH to PDH-E1α was calculated; n=4 per group. **F-G)** 1mo post-tamox treatment adult cardiomyocytes were assayed for mitochondrial OxPhos function using a Seahorse bioanalyzer to measure the oxygen consumption rate (OCR); Oligo = oligomycin, FCCP = mitochondrial protonophore, Rot/AA = rotenone + antimycin A. **G)** Maximal respiration (FCCP-Rot/AA), reserve capacity (FCCP-base), ATP production (Oligo-base), baseline respiration, and proton leak (Oligo-Rot/AA) represented as picomoles O^2/min/5k cells; n=3 mice per group. **H-J)** MCM (n=6) and MCUB-Tg x MCM (n=6) received tamoxifen (tamox; 25 mg/kg/day) for 4d and 1mo later were subjected to i.v. infusion of isoproterenol (Iso, 0–800 ng/kg) with invasive LV hemodynamic monitoring of: **H)** heart rate (beats/m), **I)** dP/dt maximum, and **J)** dP/dt minimum. *All data are shown as mean +/− SEM. **p<0.01, *p<0.05.*

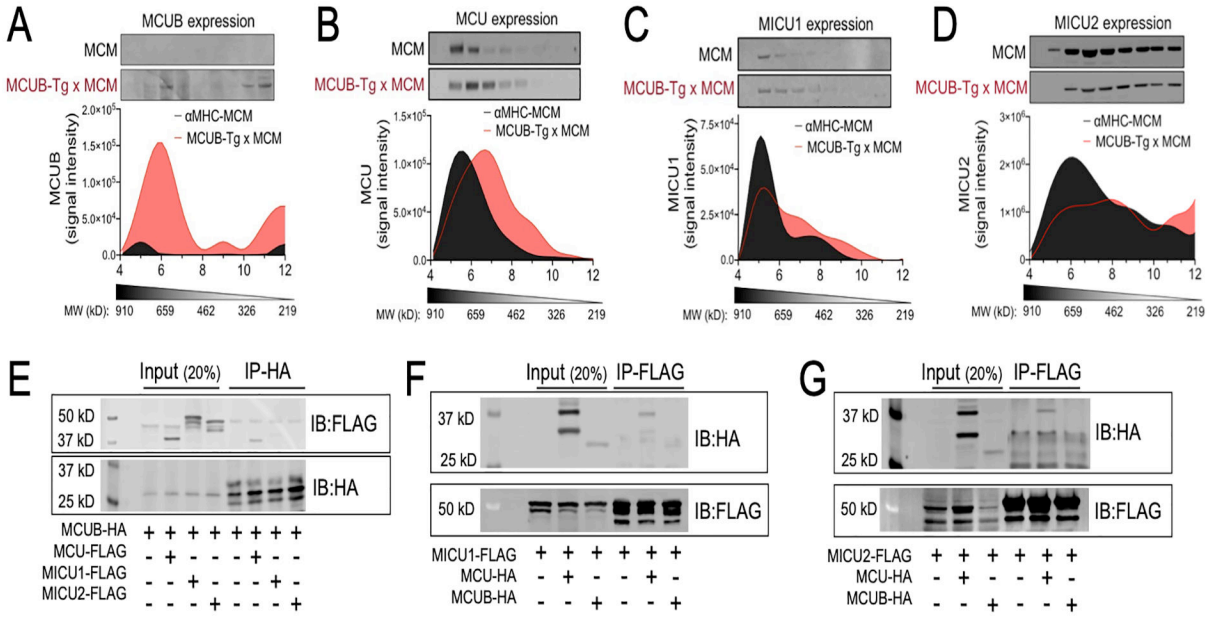

Figure 6. MCUB expression modulates mtCU stoichiometry.

A-D) Mitochondria isolated from hearts were fractionated by size-exclusion FPLC and independent fractions were immunoblotted for mtCU components. Densitometry analysis was performed and the chromatographs depict relative expression of mtCU subunits in the high-MW fractions; n=3 mice per group. All fractions were fitted to the MW of known standards. **A)** MCUB **B)** MCU **C)** MICU1 **D)** MICU2. **E)** MCUB-HA was co-transfected with MCU-FLAG, MICU1-FLAG, or MICU2-FLAG. HA-immunoprecipitation was performed and immunoblotted for FLAG and HA; n=3. **F)** MICU1-FLAG was co-transfected with MCU-HA or MCUB-HA. FLAG immunoprecipitation was performed and Western blotted for HA and FLAG; n=3. **G)** MICU2-FLAG was co-transfected with MCU-HA or MCUB-HA. FLAG immunoprecipitation was performed and probed for HA and FLAG immunoreactivity. 20% of total lysate was loaded to determine relative input.